Chem. Senses 34: 363–372, 2009
doi:10.1093/chemse/bjp013
Advance Access publication March 20, 2009

Morphological and Physiological Characteristics of the Serotonin-Immunoreactive Neuron in the Antennal Lobe of the Male Oriental Tobacco Budworm, *Helicoverpa assulta*

Xin Cheng Zhao and Bente Gunnveig Berg

Department of Psychology/Neuroscience Unit, MTFS, Norwegian University of Science and Technology (NTNU), 7489 Trondheim, Norway

Correspondence to be sent to: Bente Gunnveig Berg, Department of Psychology/Neuroscience Unit, MTFS, Norwegian University of Science and Technology (NTNU), 7489 Trondheim, Norway. e-mail: bente.berg@ntnu.no

This work was supported by the Norwegian Research Council (project no. 1141434).

Abstract

We have characterized, by intracellular recording and staining combined with immunocytochemistry, a serotonin-immunoreactive neuron in the central olfactory pathway of the male moth *Helicoverpa assulta*. The neuron joins the unique category of so-called SI antennal-lobe neurons, previously described in several insect species. In similarity with that originally discovered in the sphinx moth *Manduca sexta*, the neuron identified here has a large soma located posteriorly in the lateral cell cluster of the antennal lobe and an unbranched neurite projecting into the ipsilateral protocerebrum via the inner antennocerebral tract. After bypassing the central body, the axon crosses the midline and extends through the corresponding antennocerebral tract to the contralateral antennal lobe where it innervates the entire assembly of glomeruli including the male-specific macroglomerular complex. The neuron arborizes into several fine branches in bilateral protocerebral regions anterior to the calyces of the mushroom bodies, particularly on the contralateral side. The physiology of the neuron revealed 2 distinctly different spiking amplitudes, 1 small showing a relatively high spontaneous activity and 1 large showing low activity. The small-amplitude spikes displayed increased frequency when pheromones and plant odors were blown over the antenna. The large-amplitude spikes, which had an unusually long duration, showed no observable responses.

Key words: biogenic amine, centrifugal neuron, heliothine moth, 5-hydroxytryptamine, olfactory system, two spiking amplitudes

Introduction

More than half a century ago, Hebb (1949) suggested that the capability of learning implies particular changes in synaptic strength at the level of neural networks. Hebb proposed his idea based on experiments carried out in the marine snail *Aplysia californica*. The learning mechanisms studied in *Aplysia* involves the activation of a particular neuron type—namely, a population of modulatory neurons that releases the biogenic monoamine serotonin (5-hydroxytryptamine). These serotonergic neurons make synaptic connections with sensory neurons and interneurons in the signal pathway underlying the gill-withdrawal reflex. More precisely, serotonin activates a number of receptor subtypes that influence different K^+ currents (Klein et al. 1982; Barbas et al. 2003). In general, serotonin seems to play a prominent role as a modulator within neural networks of invertebrates, as well as vertebrates (Nässel 1988; Weiger 1997; Dickinson 2006).

Each of the 2 antennal lobes, which constitute the primary olfactory center of the insect brain, is extensively innervated by 1 serotonin-immunoreactive (SI) neuron (reviewed by Schachtner et al. 2005; Dacks et al. 2006; Kloppenburg and Mercer 2008). This unique kind of antennal-lobe neuron, thus being 1 in a pair, was originally described in the sphinx moth *Manduca sexta* (Kent et al. 1987). The remarkable morphology of the neuron, including extensive ramifications in the antennal lobe contralateral to that containing the cell body, was found to be maintained throughout all life stages including that of larvae, pupae, and imago. In fact, all holometabolous insects studied, except hymenopterans, have a pair of SI antennal-lobe neurons with a similar branching pattern (Dacks et al. 2006). Hemimetabolous insects, that is, species that undergo incomplete metamorphosis, also have a pair of SI neurons, though with ipsilateral

arborizations in the antennal lobe (Salecker and Distler 1990). Based on their unique projection patterns, the various morphological subtypes are in general suggested to serve as descending neurons that modulate olfactory information in the antennal lobe (Dacks et al. 2006). Ultrastructural studies of the SI neuron, both in moth and cockroach, have been reported to mainly express output synapses in the antennal lobe—a finding that indicates the presence of a centrifugal neuron influencing the olfactory information at the glomerular level, possibly through signals received at the protocerebral level (Salecker and Distler 1990; Sun et al. 1993).

In addition to the morphological studies, considerable evidence from functional investigations suggests that the SI neuron plays a substantial role in modulation of general olfactory information (reviewed by Kloppenburg and Mercer 2008). Whole-cell patch-clamp recordings from cultured antennal-lobe neurons of the sphinx moth have demonstrated that increased levels of serotonin causes reduction in 2 voltage-gated K^+currents, a fast, transient A-type and a slower-activating delayed-rectifier type (Mercer et al. 1995). In full accordance with these findings, in vivo recordings from antennal-lobe neurons of the same species showed that exogenously applied serotonin alters responses to afferent input by increasing membrane excitability, resistance, and duration of action potentials (Kloppenburg and Hildebrand, 1995). During the last decade, additional evidence has indicated enhancement of central olfactory neuron responses by serotonin during stimulation both with pheromones and plant odors (Kloppenburg et al. 1999; Kloppenburg and Heinbockel 2000; Hill et al. 2003; Dacks et al. 2008).

Also, behavioral studies indicate a role for serotonin as a prominent neuromodulator in the insect olfactory system. The male moths *Trichoplusia ni* and *Lymantria dispar* showed a widened time window for receptability of female-produced pheromones during raised levels of serotonin (Linn and Roelofs 1986; Linn et al. 1992). Interestingly, the serotonin level in the moth brain has a rise and fall that corresponds to the circadian fluctuation in the male's sensitivity to pheromone (Kloppenburg et al. 1999; Gatellier et al. 2004).

Although the morphology and function of the SI antennal-lobe neuron has been thoroughly studied in numerous insect species, the physiology of the neuron itself is largely unexplored. Only 1 study has so far reported about the physiological properties of this particular type of neuron. Using the intracellular recording and staining technique, performed onto a protocerebral brain region of the silk moth *Bombyx mori*, Hill et al. (2002) found that the SI neuron fired spontaneous, long-duration action potentials and responded to air puffs applied to the antenna. Here, we present morphological and physiological characteristics of the SI antennal-lobe neuron in the noctuid moth *Helicoverpa assulta*, based on 1 successful intracellular recording performed from the antennal lobe. The SI neuron that had branching profiles almost identical to those found in the sphinx moth *M. sexta*, fired 2 distinctly different types of action potentials; 1 with a small amplitude showing increased spike frequencies when odors were blown over the antenna and the other with a large, long-duration amplitude showing no observable responses.

Materials and methods

Insects and preparation

Helicoverpa assulta pupae, originating from a laboratory culture, were kindly provided by Dr Jun Feng Dong (Henan University of Science and Technology, Henan, China). Male and female pupae were separated and kept in climate chambers on reversed photoperiod 14:10 h light:dark at 22 °C. The adults were fed a 5% sucrose solution. Experiments were performed on adult males, 2–5 days after ecdysis, as described by Berg et al. (1998). The moth was restrained inside a plastic tube with the head and antennae exposed. The head was immobilized with wax (Kerr Corporation, Romulus, MI) and the antennae lifted up by needles. The brain was exposed by opening the head capsule and removing the mouth parts, the muscle tissue, and major trachea. The sheath of the antennal lobe was removed by fine forceps in order to facilitate microelectrode insertion into the tissue. Once the head capsule was opened, the brain was supplied with Ringer's solution (in mM: 150NaCl, 3$CaCl_2$, 3KCl, 25Sucrose, and 10*N*-tris (hydroxymethyl)-methyl-2-amino-ethanesulfonic acid , pH 6.9). The whole preparation was positioned so that the antennal lobes were facing upward and the ipsilateral antenna of the recording site could be stimulated with odorants.

Intracellular recording and staining

The intracellular recording from the antennal-lobe neuron was carried out as described by Berg et al. (1998). Recording electrodes were made by pulling glass capillaries (Borosilicate glass capillaries, Hilgenberg GmbH, Germany; OD: 1 mm, ID: 0.75 mm) on a horizontal puller (P97, Sutter Instruments, Novarto, CA). The tip was filled with a fluorescent dye (4% tetramethylrhodamine dextran with biotin, Micro-Ruby, Molecular Probes; Invitrogen, Eugene, OR, in 0.2 M K^+ acetate) and the glass capillary back-filled with 0.2 M K^+-acetate. A chloridized silver wire inserted into the eye served as the indifferent electrode. The recording electrode, which had a resistance of 150–400 MΩ, was lowered carefully into the antennal lobe by means of a micromanipulator (Leica, Bensheim, Germany). Neuronal spike activity was, after being amplified (AxoClamp 2B, Axon Instruments, Union, CA), monitored continuously by oscilloscope and loudspeaker. The recordings were stored by Spike2 6.02 software (Cambridge Electronic Design, Cambridge, United Kingdom).

After physiological recordings, the neuron was iontophoretically stained by receiving 2–5 nA depolarizing current pulses with 200-ms duration at 1 Hz for about 10 min via the glass capillary electrode. In order to allow neuronal transportation of the dye, the preparation was kept for

1 h at room temperature. The brain was then dissected from the head capsule. After being fixed in 4% paraformaldehyde for 1 h at room temperature, the brain was rinsed with a phosphate-buffered saline (PBS; in mM: 684NaCl, 13KCl, 50.7Na_2HPO_4, 5KH_2PO_4, pH 7.4). Staining was then intensified by incubating the brain in fluorescent conjugate streptavidin-Cy3 (Jackson Immunoresearch, West Grove, PA, diluted 1:200 in PBS), which binds to biotin, for 2 h. Incubation was followed by rinsing with PBS and dehydration in an ascending ethanol series (50%, 70%, 90%, 96%, 2 × 100%; 10 min each). Finally, the brain was cleared and mounted in methylsalicylate.

Stimulation

The odor delivery system for the intracellular recording consisted of 2 glass cartridges placed side by side, both pointing toward the antenna at a distance of 2 cm. One replaceable cartridge contained a piece of filter paper onto which a particular odor stimulus was applied. The other cartridge was empty. An airflow (500 mL/min) led through 1 of the 2 cartridges was continuously blown over the antenna. During each stimulus period, which lasted for 400 ms, the airflow was switched by a valve system from the empty cartridge to the odor-bearing cartridge.

Based on previous electrophysiological investigations that have identified the ligands for 3 types of male-specific receptor neurons and for a number of plant odor neuron types (Berg and Mustaparta 1995; Stranden et al. 2003; Røstelien et al. 2005), the following stimuli were used: the primary pheromone component *cis*-9-hexadecenal (Z9-16:AL), the secondary pheromone component *cis*-11-hexadecenal (Z11-16:AL), the interspecific signal *cis*-9-tetradecenal (Z9–14:AL), the binary pheromone mixture of Z9-16:AL and Z11-16:AL in the ratio 95:5 (all insect produced substances delivered by Plant Research International, Pherobank, Wageningen, NL), and the plant oil ylang–ylang (Dragoco, Totowa, NJ). Each compound, which was diluted in hexane, was applied onto a small filter paper. The hexane was allowed to evaporate before the filter paper was wrapped up and placed in the cartridge. All stimuli were prepared so that the filter paper contained a particular dose of each odorant, that is, 1 ng of the single insect-produced substances, 1 and 10 ng of the binary pheromone mixture, and 100 μg of the plant oil.

Immunocytochemistry

After having analyzed the iontophoretically stained neuron by confocal laser scanning microscopy, the brain was rehydrated through a decreased ethanol series. Then the brain was embedded in gelatin/albumin, postfixed in 4% buffered formaldehyde for 17 h at 4 °C, and sectioned at 40 μm with a vibrating blade microtome (Leica VT 1000S; Leica, Nussloch, Germany). Vibratome sections were collected and washed in a phosphate-buffered saline containing 0.5% Triton X-100 (PBSX; 0.1 M, pH 7.4) 3 × 10 min at room temperature. To minimize nonspecific staining, the sections were incubated with 5% normal goat serum (NGS; Sigma, St. Louis, MO) for 1 h at room temperature. The sections were then incubated in the primary antibody, rabbit antiserum against serotonin (Immunostar, Hudson, WI; dilution 1:2000 in PBSX containing 5% NGS), for 20 h at 4 °C. After being rinsed in PBSX 3 × 10 min at 4 °C, the sections were incubated with Cy5-conjugated antirabbit secondary antibody (Invitrogen; dilution 1:200 in PBSX) for 20 h at 4 °C. Finally, after being rinsed again, the sections were mounted on gelatin-coated glass slides, dehydrated, cleared in xylene, and mounted in Permount under a glass coverslip. In addition to the iontophoretically stained preparation, immunolabeling experiments were carried out on 5 unprocessed brains in order to verify the morphology of the SI antennal-lobe neuron.

Preadsorption experiments on *H. assulta* brain tissue were carried out by applying a conjugate control for serotonin, that is, lyophilized serotonin creatine sulfate coupled to bovine serum albumin (Immunostar, Hudson, WI) at a concentration of 20 μg/mL. Thus, the peptide was added to the antiserum prior to its application to the sections.

Confocal microscopy, image processing, and data analyses

Serial optical images were acquired by using a confocal laser scanning microscope (LSM 510, META Zeiss, Jena, Germany) with a 40× and a 63× objective (C-Achroplan 40×/0.8W; C-Apochromat 63×/1.2W corr). The intracellular staining obtained from the fluorescence of rhodamine/Cy3 (Ex_{max} 550 nm, Em_{max} 570 nm), was excited by the 543-nm line of a HeNe1 laser and the immunostaining, obtained from the Cy5 (Ex_{max} 682 nm, Em_{max} 647 nm), was excited by the 633-nm line of a HeNe2 laser. The distance between each section was 2 μm. The pinhole size was 1 and the resolution 1024 × 1024 pixels. Optical sections from confocal stacks were reconstructed by using the projection tool of LSM 510. Adobe Photoshop CS2 (Adobe System, San Jose, CA) was used in order to adjust brightness and contrast. The images were finally edited in Adobe Illustrator CS2.

The electrophysiological recording was stored and analyzed by the use of the Spike2 program. The spontaneous activity of each amplitude type was measured by counting the number of spikes during the 1-s period before each stimulation onset, that is, over a total period of 7 s. The duration of each action potential category was calculated by measuring the width, at the baseline level, of 35 spikes.

Results

Morphology of the iontophoretically stained neuron

We identified, through 1 intracellular recording and staining experiment, a neuron that is morphologically similar to the SI antennal-lobe neuron initially described in *M. sexta* (Kent et al. 1987; Figure 1). The neuron has a large soma located

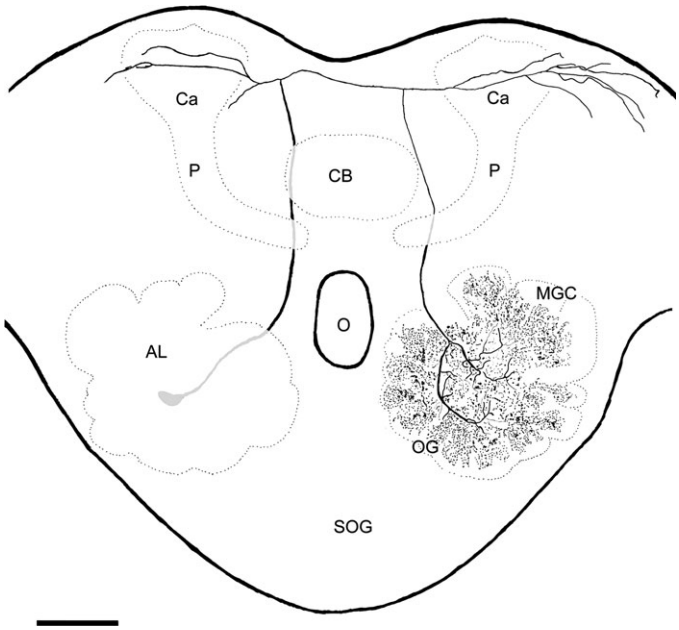

Figure 1 Complete reconstruction of the intracellularly stained SI antennal-lobe neuron made from 6 stacks of confocal images acquired with the 40× objective. The frontally oriented brain was tilted slightly dorsally. From the large cell body located posteriorly in one antennal lobe (AL), the primary neurite projects via the IACT to the superior protocerebrum where it bifurcates. One fiber gives off a few fine branches in an area anterior to the calyces (Ca). The second fiber crosses the midline and targets the contralateral protocerebrum including an area anterior to the calyces and a more laterally positioned region. The horizontal fiber that crosses the midline gives off a second branch projecting via the IACT to the contralateral antennal lobe. Here, it innervates the entire assembly of glomeruli including the 3 units of the MGC and the numerous ordinary glomeruli (OG). CB = central body, O = esophagus, and P = pendunculus. Scale bar = 100 μm.

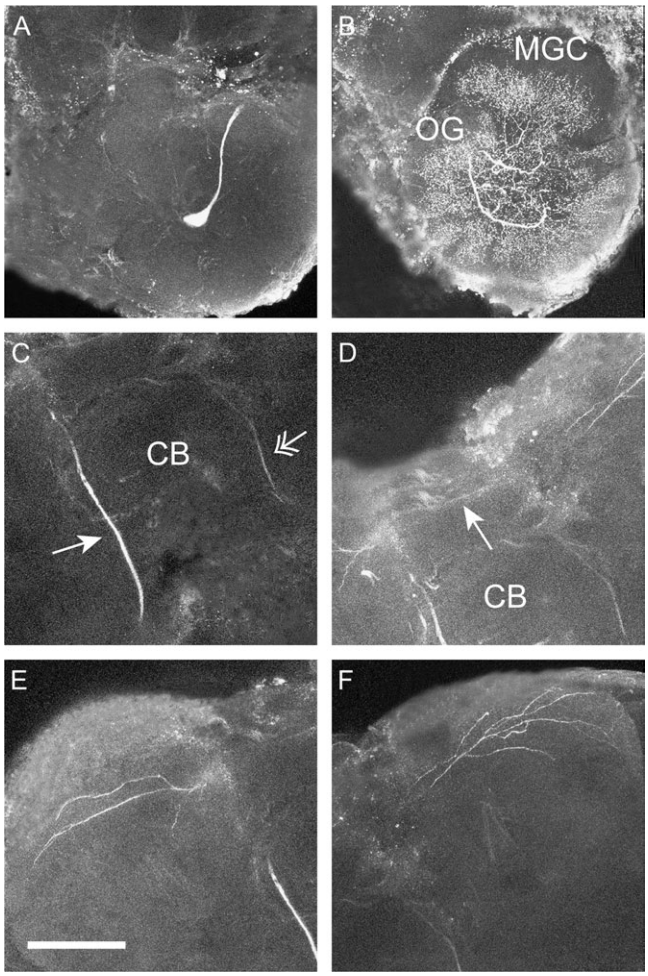

Figure 2 Confocal images of the iontophoretically stained SI antennal-lobe neuron (same confocal images as used for the reconstruction in Figure 1). The images are reconstructions of several sections. **(A)** A large cell body attached to a naked primary neurite is located in one antennal lobe. **(B)** In the contralateral antennal lobe the neuron extensively innervates all glomeruli including the units of the MGC and the numerous ordinary glomeruli (OG). **(C)** The neuron connects the two antennal lobes through a long loop consisting of a primary neurite (arrow) projecting from the ipsilateral antennal lobe to the protocerebrum via the IACT and a descending fiber (double arrow) passing from the protocerebrum to the contralateral antennal lobe via the counterpart IACT. The 2 fiber segments of the neuron are visible as they bypass the central body (CB). **(D)** A thin branch of the neurite crosses the midline and projects from the medial part of the ipsilateral superior protocerebrum to the contralateral protocerebrum (arrow). **(E,F)** The neuron arborizes into several fine profiles in bilateral regions of the superior protocerebrum, particularly on the contralateral side (F). Scale bar = 100 μm.

posteriorly in the lateral cell cluster of one antennal lobe and extensive arborizations in the contralateral antennal lobe (Figures 1 and 2A,B). The primary neurite exits the antennal lobe and bypasses the central body through the inner antennocerebral tract (IACT; Figure 2C). In the superior part of the medial protocerebrum, it bifurcates; one branch crosses the midline (Figure 2D), and the other projects into the ipsilateral protocerebrum where it gives off arborizations anterior to the calyces of the mushroom body (Figures 1 and 2E). The fiber crossing the midline bifurcates further; one branch arborizes in the protocerebrum, more precisely in an area corresponding to that innervated in the counterpart hemisphere, plus the adjacent lateral protocerebrum (Figures 1 and 2F). The second branch projects anteriorly via the IACT (Figure 2C) into the contralateral antennal lobe where it innervates the inner region of all glomeruli including the 3 units of the macroglomerular complex (MGC) and the numerous ordinary glomeruli (Berg et al. 2002; Figures 2B and 3). As compared with the few fine extensions appearing in the protocerebrum, the numerous profiles in the antennal lobe are widespread and partly granular (Figure 3). No branches were present in the ipsilateral antennal lobe.

Immunocytochemistry

Immunostaining with antiserum against serotonin proved that the iontophoretically stained neuron was identical to the SI antennal-lobe neuron. As shown in Figure 4A–A″, the iontophoretically stained soma in the ipsilateral antennal lobe was immunoreactive against the serotonin antiserum. The thick neural branches in the contralateral antennal lobe were also

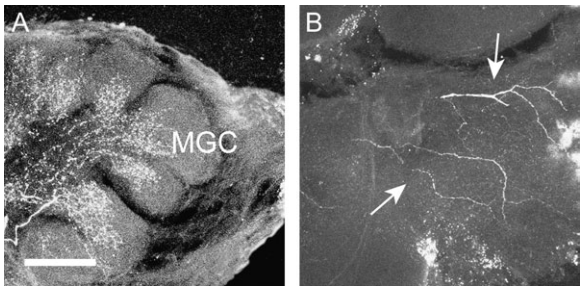

Figure 3 High magnification images of iontophoretically stained branches in the antennal lobe and the protocerebral region of the contralateral hemisphere (obtained with the 63× objective). The images are reconstructions of several sections, that is, 15 and 11 sections for **(A)** and **(B)**, respectively. (A) The 3 units of the MGC, plus surrounding glomeruli of the ordinary type are extensively innervated by numerous grainy branches that are restricted to the basal region of each glomerulus. (B) The neural branches in the protocerebrum (arrows) are relatively few and slender. Scale bar: 50 μm.

double labeled (Figure 4B–B″,C–C″), likewise the bilateral projections in the protocerebrum (Figure 4D–D″,E–E″). Parts of the axon and the fine glomerular arborizations showed no immunoreactivity. The presence of a paired SI antennal-lobe neuron, constituting the matching part of the intracellularly stained neuron, was revealed by neural elements showing immunolabeling but no double labeling, that is, a large soma residing within the contralateral antennal lobe (Figure 4C′,C″) and thick branching profiles located in the counterpart antennal lobe (Figure 4A′,A″). Serotonin immunostaining alone, performed on 5 additional brains, also showed a pair of immunoreactive antennal-lobe neurons, each with a branching pattern similar to that of the iontophoretically stained neuron (data not shown). The preadsorption experiments showed a complete lack of immunoreactivity in all regions of the brain treated with the conjugate control (data not shown).

Physiology of the intracellularly stained SI neuron

The recording was performed from the neural branches located in the antennal lobe contralateral to that housing the cell body. Spontaneously firing action potentials from 2 distinctly different types of spiking amplitudes were measured (Figure 5A). A small-amplitude spike (~10 mV) showed a high spontaneous activity (~13.3 Hz) and a large-amplitude spike (~40 mV) showed a low activity (~1.3 Hz). The large spikes had a duration of 10.9 ± 1.2 ms (mean ± SD [standard deviation], $n = 35$) and the small spikes a duration of 3.3 ± 0.4 ms (mean ± SD, $n = 35$; Figure 5C,D).

The small-amplitude spikes showed excitatory responses to all stimuli applied to the antenna by displaying spike frequencies in the range of 24–42 Hz during the 1-s period after stimulus onset (Figure 5A,B). Pure air was not tested. As demonstrated in Figure 5A,B, the binary pheromone blend (at high concentration) and the plant odor ylang–ylang elicited higher spike frequencies than the remaining stimuli. In general, the responses outlasted the stimulation period and had a mean latency of 139.8 ± 64.73 ms (mean ± SD, $n = 7$). Regarding the large-amplitude spikes, slightly increased frequencies occurred during some of the stimulation periods, but no visible responses appeared (Figure 5A–).

Discussion

Morphology—comparison with other moth species

Several structural characteristics of the neuron presented here—including a large soma residing within the posterolateral region of the antennal lobe, a primary neurite crossing the brain midline posterior to the central body, collaterals extending into bilateral areas of the protocerebrum, and extensive innervations in the contralateral antennal lobe—is in full agreement with corresponding morphological data achieved from investigations of other moth species (Kent et al. 1987; Hill et al. 2002; Dacks et al. 2006). Also the characteristic branching pattern in the antennal lobe, that is, profiles restricted to the basal region of each glomerulus (Figure 3A), is in accordance with results from other moths. Double-labeling experiments in *M. sexta* have demonstrated a lack of overlap between the sensory axons and SI processes (Sun et al. 1993). Corresponding double-labelings have not been carried out in *H. assulta*, but the target area of the neural terminals presented here differs from that of the sensory neurons which are reported to project in the peripheral layer of the glomeruli (Berg et al. 2005).

With one exception, all previous studies have based their morphological data on immunocytochemistry only. The exceptional case concerns the investigation of the SI antennal-lobe neuron in the silk moth *B. mori* where intracellular staining with a fluorescent dye was used, that is, the same technique as utilized here (Hill et al. 2002). The iontophoretic stains in the silk moth revealed extensive branches in brain regions that had not been reported in immunocytochemical studies of corresponding neurons in other insect species, as for instance the sphinx moth *M. sexta*. These additional regions, some of which were not stained by the immunolabeling technique in the silk moth either, include the antennal lobe and the lateral accessory lobe of the ipsilateral hemisphere, plus the calyces of the mushroom bodies (Hill et al. 2002). The iontophoretic stains of the SI antennal-lobe neuron revealed here, lack neural branches in all these areas. Because the same staining technique was used in the investigation of the SI neuron in *H. assulta* and *B. mori*, it seems as though the variations in morphology arise from species-specific characteristics. Interestingly, the branching pattern found here is similar to that of the SI antennal-lobe neuron originally described in *M. sexta* (Kent et al. 1987; Dacks et al. 2006). As in the sphinx moth, a naked cell body and an unbranched primary neurite reside within the antennal lobe. The lack of arborizations in the calyces and the lateral accessory lobe is also in accordance with the findings in *M. sexta.* The only distinction between the sphinx moth and the heliothine moth

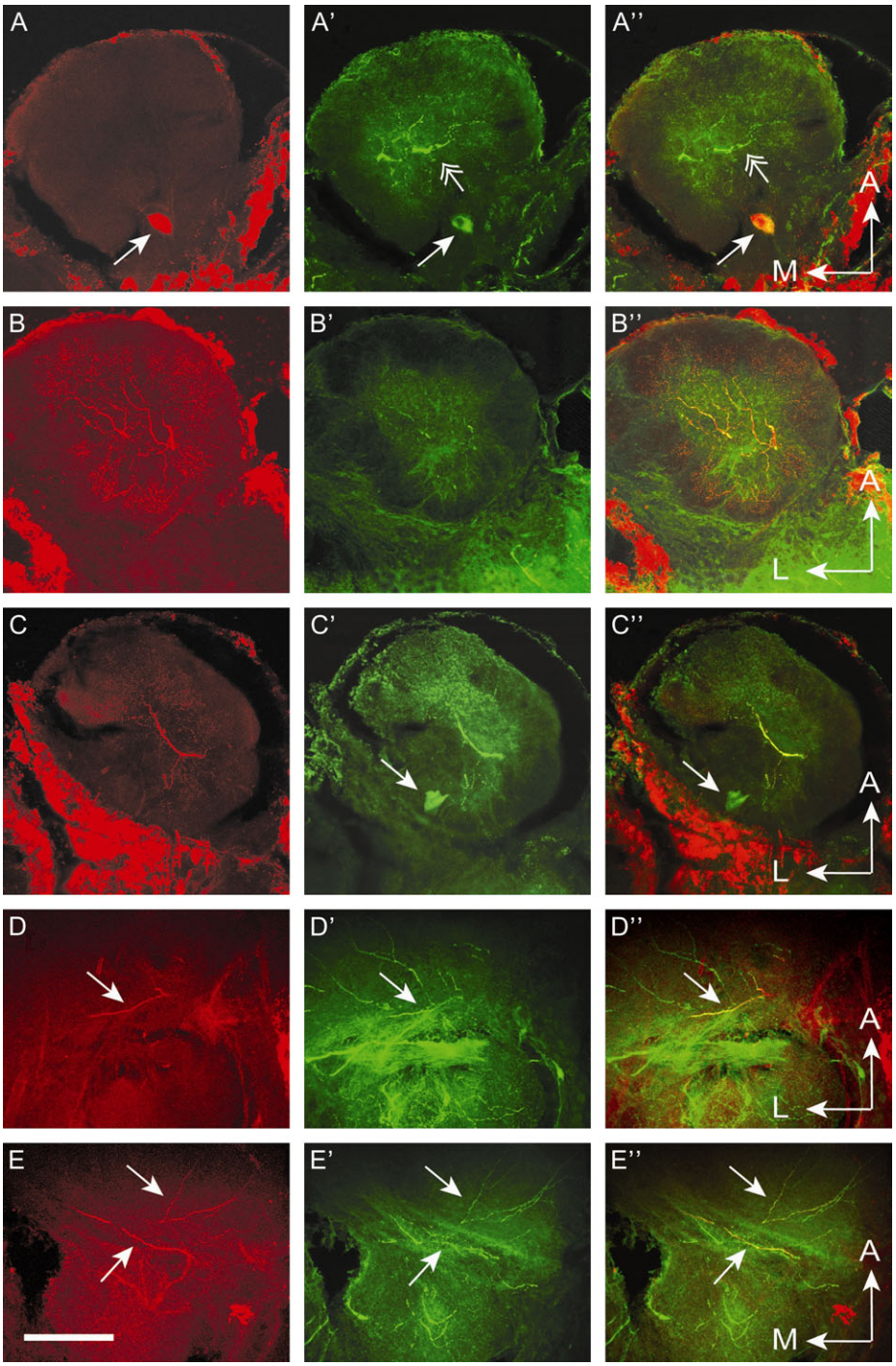

Figure 4 Confocal images of the paired antennal lobes and the bilateral protocerebral regions acquired by use of 2 different staining techniques. The images in each row, which originate from the same stack, include 6–18 optical sections. Left: Intracellular staining (red). Middle: Immunostaining (green). Right: Overlay. The upper row shows images from the ipsilateral antennal lobe, the 2 subsequent rows images at various depths of the contralateral antennal lobe, and the 2 lower rows images from protocereral areas in the two hemispheres, respectively. **(A–A″)** Images of the ipsilateral antennal lobe containing the double-labeled soma of the serotonin-immunoreactive (SI) antennal-lobe neuron. Left: The iontophoretically stained soma (red; arrow). Middle: One immunoreactive soma (green; arrow). Right: One double-labeled soma (orange; arrow). The immunostained branches belong to the counterpart SI neuron and are therefore not double labeled (double arrows). **(B–B″,C–C″)** Two image series at various depths of the contralateral antennal lobe show double-labeled arborizations belonging to the SI neuron. Left: Iontophoretically stained arborizations include thick branches in the central coarse neuropil and finer profiles in the glomeruli (red). Middle: Thick branches in the coarse neuropil show immunoreactivity (green). Right: The thick branches in the central course neuropil are double labeled (orange/yellow). The immunostained soma in (C′,C″) belongs to the counterpart SI neuron and is therefore not double labeled (arrows). **(D–D″,E–E″)** Two image series, each from one hemisphere, showing double-labeled branches in the protocerebrum. Left: iontophoretically stained extensions in the ipsilateral (D) and contralateral (E) protocerebrum (red; arrows). Middle: fine profiles showing immunoreactivity in the ipsilateral (D) and contralateral (E) protocerebrum (green; arrows). Right: branches showing double labeling in the ipsilateral (D) and contralateral (E) protocerebrum (yellow; arrows). A = anterior, M = medial, and L = lateral. Scale bar = 100 μm.

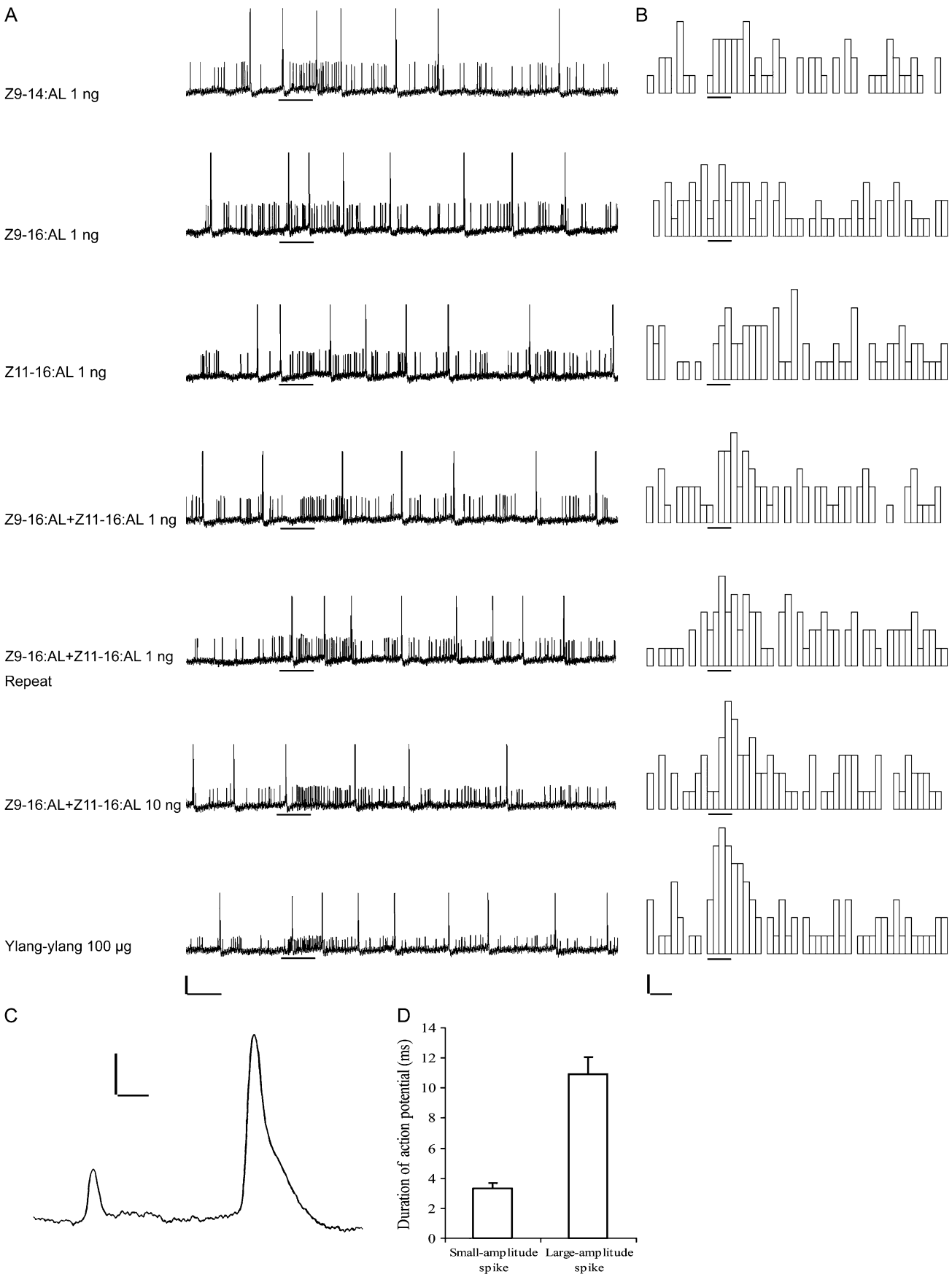

is the neural innervation pattern in the central body. The SI neuron of *M. sexta* is reported to have fine neural branches in the central body (Kent et al. 1987), a finding that also applies to *B. mori* (Hill et al. 2002). In the heliothine moth, however, no such profiles were found. An alternative explanation for the morphological discrepancies reported could be incomplete labeling of the neuron in some specimens. Regarding the data presented here, we cannot exclude the possibility that a prolongation of the incubation time in strepdavidin-Cy3 would visualize fine neural branches in additional neuropil regions.

Physiological properties

The electrophysiological recording performed here measured action potentials from 2 distinctly different types of spiking amplitudes, a small-amplitude spike showing a relatively high spontaneous activity and a large-amplitude spike showing a low activity. Based on the recording technique, it is reasonable to assume that both spike categories originate from the same neuron. Alternatively, the different amplitudes could arise from 2 electrically coupled neurons. There is no evidence however for the presence of gap junctions in glomerular neuropil of the moth antennal lobe (Tolbert and Hildebrand 1981). Also, the solitary labeled soma, as demonstrated here, indicates that both spiking amplitude types originate from the SI antennal-lobe neuron. Different spikes in the same recording were previously observed in many local antennal-lobe neurons of the sphinx moth (Matsumoto and Hildebrand 1981; Christensen et al. 1993). Their appearance was suggested to originate from various spike initiating zones of the neuron.

Due to the fact that the electrophysiological data from the present study are based on 1 experiment only, the possibility of making quantitative analyses is limited. However, of the 2 amplitude types recorded, the small type obviously responded to airborne stimuli applied to the antenna. As shown in Figure 5, the small spikes constantly increase their frequency when the antenna is stimulated by an odor puff. Unfortunately, pure air was not tested, and therefore, it might well be that the small-amplitude spikes in fact respond to mechanical stimulation. Nevertheless, the stronger response to certain odor stimuli obtained here—like the pheromone blend and ylang-ylang oil—indicates that there might be a distinct olfactory response. Interestingly, another centrifugal antennal-lobe neuron recently identified in the heliothine moth showed specific responses to odor stimuli and pure air (unpublished data).

The large spikes recorded in the present study are strikingly similar to the action potentials of the SI antennal-lobe neuron (#1) previously reported in *B. mori* (Hill et al. 2002). Both have a characteristic shape with a large-amplitude spike of about 40 mV and an unusually long duration of about 10 ms (10.9 in *H. assulta* and 9.3 ms in *B. mori*). The frequencies of their spontaneous activities are also comparable, being about 1.3 and 3 Hz in the two species, respectively. In similarity to the findings in the silk moth, the large spikes recorded here did not respond to olfactory stimulation. The lack of mechanical responses, however, differs from that reported in the silk moth where an air puff blown over the antenna induced a response (Hill et al. 2002). This discrepancy could be due to slightly different stimulation systems utilized in the two experimental setups. In the present study, the stimuli were applied within intervals of a continuous airflow, whereas Hill et al. presented the stimuli without an intermittent airflow. The large-amplitude spikes of the heliothine moth may therefore have failed to respond because of persistent stimulation. Based on the atypical spike duration, it may be speculated whether the large action potential type is driven by an ionic mechanism distinct from the common type that involves sodium and potassium. Interestingly, calcium-dependent action potentials with a duration of 7–20 ms have previously been recorded from neurosecretory cells of insects (Orchard 1976; Ichikawa 2001). In general, long-duration action potentials have been suggested to serve particular purposes in neural propagation, more precisely to ensure that the signals are maintained and forwarded at branching points where the axon diameter increases (Westerfield et al. 1978). As in moths and other invertebrates, there is also a scarcity of knowledge concerning physiological properties of serotonergic neurons in vertebrates. Electrophysiological investigations of pontomedullary serotonergic neurons in the rat, however, have reported a particularly low discharge rate of 1.8 Hz (Mason 1997), which is similar to the spontaneous activity measured in the present investigation. Another study, also in rat, found that spinally projecting serotonergic neurons displayed a particularly large action potential half width (Zhang et al. 2005), a finding that also corresponds to the results presented here.

Whereas the present recording was carried out from the antennal lobe, the recordings in the silk moth were performed from the lateral accessory lobe of the protocerebrum. As reported by Hill et al. (2002), the signals from the protocerebral region included only 1 amplitude category. The

Figure 5 Physiological properties of the intracellularly stained SI antennal-lobe neuron. **(A)** The neuron fired spontaneous action potentials by displaying 2 distinctly different spiking amplitudes, a small-amplitude spike showing a relatively high activity and a large-amplitude spike showing low activity. The small-spiking amplitude responded with an excitatory response to all stimuli tested. The responses to the binary pheromone blend and to the plant oil ylang–ylang were stronger than the responses to the remaining stimuli. The large-spiking amplitude showed no observable responses to any of the tested stimuli. Stimulus onset is indicated below the recording. Scale bars = 10 mV, 400 ms. **(B)** Histograms showing spike frequencies of the small-amplitude type before and after stimulation onset. Each bin represents the frequency during a period of 100 ms. Scale bars = 10 Hz, 400 ms. **(C)** Part of the recording sequence showing the waveforms of the 2 action potential categories, 1 of which displays a relatively great width. Scale bars = 10 mV, 5 ms. **(D)** Histograms showing the mean duration and SD of each action potential type (n = 35).

appearance of 1 amplitude type rather than 2 may therefore be caused by the different recording sites, which would indicate that the small spiking type is confined to the antennal lobe. The ultrastructural investigation performed by Sun et al. (1993) proposed that the SI antennal-lobe neuron may serve dual functions based on the finding of both input and output synapses in the antennal lobe of the sphinx moth. The presence of both input and output synapses have also been reported in the primary olfactory center of cockroach (Salecker and Distler 1990). The neural responses observed here, which arise from stimulation applied onto the antenna, are presumably mediated through a kind of input channel in the antennal lobe. Based on present and previous findings, we may speculate whether the 2 spiking types that appear here originate in different zones of this widespread neuron. The large-amplitude spikes are possibly initiated in the bilateral protocerebral regions and provide, from a distance, the presumed feedback mechanism in the antennal lobe, whereas the small-amplitude spikes are initiated in the antennal-lobe glomeruli where they serve in local processing of olfactory information. The seeming paradox that the locally generated spikes are the small type could be due to morphological properties of the neural branches in the antennal lobe. It is well known that action potentials in general change their shape and velocity according to the geometry of the neural conductor (Goldstein and Rall 1974; Stuart et al. 1997; Debanne 2004). Spikes initiated in fine distal dendrites may be attenuated and possibly die out as they propagate in the forward direction along neural profiles of increasing diameter (Häusser et al. 2000). Based on the glomerular ramification pattern of the SI neuron, that is, thin peripheral branches interconnected via thick central branches, it is conceivable that this particular neuron is capable of generating not only spikes confined to the antennal lobe but also spikes that act locally within distinct glomeruli. In similarity to previous findings in olfactory bulb mitral cells, such an arrangement could establish distal dendritic regions acting independently of each other (Chen et al. 2002). As regards the modulatory capability of the widespread SI antennal-lobe neuron, we can imagine that the coincidence of particular events, small spikes acting locally and large spikes acting globally, is of particular significance.

Funding

Norwegian Research Council (project no. 1141434).

Acknowledgements

We are grateful to Dr Jun Feng Dong (Henan University of Science and Technology, Henan, China) for sending pupae regularly, to Professor Linda White (Norwegian University of Science and Technology, NTNU) for correcting the language, and to Gerit Pfuhl (NTNU) for fruitful discussions. Furthermore, we thank 2 anonymous reviewers for constructive suggestions.

References

Barbas D, DesGroseillers L, Castellucci VF, Carew TJ, Marinesco S. 2003. Multiple serotonergic mechanisms contributing to sensitization in *Aplysia*: evidence of diverse serotonin receptor subtypes. Learn Mem. 10:373–386.

Berg BG, Almaas TJ, Bjaalie JG, Mustaparta H. 1998. The macroglomerular complex of the antennal lobe in the tobacco budworm moth *Heliothis virescens*: specified subdivision in four compartments according to information about biologically significant compounds. J Comp Physiol A. 183:669–682.

Berg BG, Almaas TJ, Bjaalie JG, Mustaparta H. 2005. Projections of male-specific receptor neurons in the antennal lobe of the oriental tobacco Budworm moth, *Helicoverpa assulta*: a unique glomerular organization among related species. J Comp Neurol. 486:209–220.

Berg BG, Galizia CG, Brandt R, Mustaparta H. 2002. Digital atlases of the antennal lobe in two species of tobacco moths, the oriental *Helicoverpa assulta* (male) and the American *Heliothis virescens* (male and female). J Comp Neurol. 446:123–134.

Berg BG, Mustaparta H. 1995. The significance of major pheromone components and interspecific signals as expressed by receptor neurons in the oriental tobacco budworm moth, *Helicoverpa assulta*. J Comp Physiol A. 177:683–694.

Chen WR, Shen GY, Sheperd GM, Hines ML, Midtgaard J. 2002. Multiple modes of action potential initiation and propagation in mitral cell primary dendrite. J Neurophysiol. 88:2755–2764.

Christensen TA, Waldrop BR, Harrow ID, Hildebrand JG. 1993. Local interneurons and information processing in the olfactory glomeruli of the moth *Manduca sexta*. J Comp Physiol A. 173:385–399.

Dacks AM, Christensen TA, Hildebrand JG. 2008. Modulation of olfactory information processing in the antennal lobe of *Manduca sexta* by serotonin. J Neurophysiol. 99:2077–2085.

Dacks AM, Christensen TA, Hildebrand JG. 2006. Phylogeny of a serotonin-immunoreactive neuron in the primary olfactory center of the insect brain. J Comp Neurol. 498:727–746.

Debanne D. 2004. Information processing in the axon. Nat Rev Neurosci. 5:304–316.

Dickinson PS. 2006. Neuromodulation of central pattern generators in invertebrates and vertebrates. Curr Opin Neurobiol. 16:604–614.

Gatellier L, Nagao T, Kanzaki R. 2004. Serotonin modifies the sensitivity of the male silkmoth to pheromone. J Exp Biol. 207:2487–2496.

Goldstein SS, Rall W. 1974. Changes of action potential shape and velocity for changing core conductor geometry. Biophys J. 14:731–757.

Häusser M, Spruston N, Stuart GJ. 2000. Diversity and dynamics of dendritic signaling. Science. 290:739–744.

Hebb D. 1949. The organization of behavior. New York: Wiley.

Hill ES, Iwano M, Gatellier L, Kanzaki R. 2002. Morphology and physiology of the serotonin-immunoreactive putative antennal lobe feedback neuron in the male silkmoth *Bombyx mori*. Chem Senses. 27:475–483.

Hill ES, Okada K, Kanzaki R. 2003. Visualization of modulatory effects of serotonin in the silkmoth antennal lobe. J Exp Biol. 206:345–352.

Ichikawa T. 2001. Ultradian firing rhythm of neurosecretory cells producing an insulin-related peptide in the silkmoth *Bombyx mori*. Zool Sci. 18:151–158.

Kent KS, Hoskins SG, Hildebrand JG. 1987. A novel serotonin-immunoreactive neuron in the antennal lobe of the sphinx moth *Manduca sexta* persists throughout postembryonic life. J Neurobiol. 18:451–465.

Klein M, Camardo J, Kandel ER. 1982. Serotonin modulates a specific potassium current in the sensory neurons that show presynaptic facilitation in *Aplysia*. Proc Natl Acad Sci USA. 79:5713–5717.

Kloppenburg P, Ferns D, Mercer AR. 1999. Serotonin enhances central olfactory neuron responses to female sex pheromone in the male sphinx moth *Manduca sexta*. J Neurosci. 19:8172–8181.

Kloppenburg P, Heinbockel T. 2000. 5-hydroxytryptamine modulates pheromone-evoked local field potentials in macroglomerular complex of the sphinx moth *Manduca sexta*. J Exp Biol. 203:1701–1709.

Kloppenburg P, Hildebrand JG. 1995. Neuromodulation by 5-hydroxytrptamine in the antennal lobe of the sphinx moth *Manduca Sexta*. J Exp Biol. 198:603–611.

Kloppenburg P, Mercer AR. 2008. Serotonin modulation of moth central olfactory neurons. Annu Rev Entomol. 53:179–190.

Linn CE, Campbell MG, Roelofs WL. 1992. Photoperiod cues and the modulatory action of octopamine and 5-hydroxytryptamine on locomotor and pheromone response in male gypsy moths, *Lymantria dispar*. Arch Insect Biochem Physiol. 20:265–284.

Linn CE, Roelofs WL. 1986. Modulatory effects of octopamine and serotonin on male sensitivity and periodicity of response to sex-pheromone in the cabbage looper moth, *Trichoplusia ni*. Arch Insect Biochem Physiol. 3:161–171.

Mason P. 1997. Physiological identification of pontomedullary serotonergic neurons in the rat. J Neurophysiol. 77:1087–1098.

Matsumoto SG, Hildebrand JG. 1981. Olfactory mechanism in the moth *Manduca sexta*: response characteristics and morphology of central neurons in the antennal lobes. Proc R Soc Lond B. 213:249–277.

Mercer AR, Hayashi JH, Hildebrand JG. 1995. Modulatory effects of 5-hydroxytryptamine on voltage-activated currents in cultured antennal lobe neurons of the sphinx moth *Manduca sexta*. J Exp Biol. 198:613–627.

Nässel DR. 1988. Serotonin and serotonin-immunoreactive neurons in the nervous system of insects. Prog Neurobiol. 30:1–85.

Orchard I. 1976. Calcium dependent action potentials in a peripheral neurosecretory cell of the stick insect. J Comp Physiol A. 112:95–102.

Røstelien T, Stranden M, Borg-Karlson A-K, Mustaparta H. 2005. Olfactory receptor neurons in two heliothine moth species responding selectively to aliphatic green leaf volatiles, aromatics, monoterpenes and sesquiterpenes of plant origin. Chem Senses. 30:443–461.

Salecker I, Distler P. 1990. Serotonin-immunoreactive neurons in the antennal lobes of the American cockroach *Periplaneta americana*: light- and electron-microscopic observations. Histochemistry. 94: 463–473.

Schachtner J, Schmidt M, Homberg U. 2005. Organization and evolutionary trends of primary olfactory brain centers in Tetraconata (Crustacea + Hexapoda). Arth Struct Dev. 34:257–299.

Stranden M, Røstelien T, Liblikas I, Almaas TJ, Borg-Karlson A-K, Mustaparta H. 2003. Receptor neurones in three heliothine moths responding to floral and inducible plant volatiles. Chemoecology. 13: 143–154.

Stuart G, Schiller J, Sakmann B. 1997. Action potential initiation and propagation in rat neocortical pyramidal neurons. J Physiol. 505: 617–632.

Sun XJ, Tolbert LP, Hildebrand JG. 1993. Ramification pattern and ultrastructural characteristics of the serotonin-immunoreactive neuron in the antennal lobe of the moth *Manduca sexta*: a laser scanning confocal and electron microscopic study. J Comp Neurol. 338:5–16.

Tolbert LP, Hildebrand JG. 1981. Organization and ultrastructure of glomeruli in the antennal lobes of the moth *Manduca sexta*: a study using thin sections and freeze-fracture. Proc R Soc Lond B. 213:279–301.

Weiger WA. 1997. Serotonergic modulation of behaviour: a phylogenetic overview. Biol Rev. 72:61–95.

Westerfield M, Joyner RW, Moore JW. 1978. Temperature-sensitive conduction failure at axon branch points. J Neurophysiol. 41:1–8.

Zhang L, Sykes KT, Buhler AV, Hammond DL. 2005. Electrophysiological heterogenity of spinally projecting serotonergic and nonserotonergic neurons in the rostral ventromedial medulla. J Neurophysiol. 95:1853–1863.

Accepted February 19, 2009